

PASSIVELY Q-SWITCHED Ho:YAG CERAMIC LASER WITH A GaAs SATURABLE ABSORBER

Deqing Niu,¹ Lingyu Jiang,¹ Qixiao Sui,¹ Qingliang Zhang,² Yingjie Shen,¹
and Ruijun Lan^{1*}

¹*School of Physics and Electronic Information, Yantai University
Yantai 264005, China*

²*Casivision Artificial Intelligence (Yantai) Industry Research Institute
Yantai 265400, China*

*Corresponding author e-mail: lanruijun1@163.com

Abstract

We report on a passively *Q*-switched 2 μm Ho:YAG ceramic laser, using pure GaAs as a saturable absorber. At an absorbed pump power of 1.28 W, the highest pulse repetition rate, shortest pulse width, largest single pulse energy, and highest peak power are measured to be 295 kHz, 83 ns, 1.49 μJ and 17.95 W, respectively. To the best of our knowledge, this is the first 2 μm passively *Q*-switched laser with a pure GaAs absorber, the three-photon absorption is believed to play an important role in the saturable absorption process.

Keywords: passive *Q*-switched lasers, multiphoton absorption, GaAs.

1. Introduction

2 μm lasers can be generated from Tm^{3+} and Ho^{3+} (Rare-Earth-ion-doped) laser materials, which can find practical use in optical communications, coherent laser radar, atmospheric sensing, surgery, etc. [1–3]. The greater emission cross section and longer upper-level lifetime make Ho^{3+} -doped materials preferable to Tm^{3+} -doped materials in 2 μm pulsed laser applications [4, 5]. Among the Ho^{3+} -doped crystals, YAG crystal stands out as an ideal material, owing to its high thermal conductivity and excellent mechanical properties. With the development of the sintering technology, large size Ho:YAG ceramics can be easily grown [6, 7]. Compared with Ho:YAG crystal, Ho:YAG ceramics exhibit superior thermal conductivity, higher optical uniformity, and greater damage resistance, rendering them highly promising for applications in passively *Q*-switched (PQS) lasers [8, 9].

PQS technology utilizing a saturable absorber (SA) represents an efficient method to obtain pulsed lasers. As a robust SA, GaAs has been widely used in 1 μm wavelength band [10, 11]. The photon energy of 1 μm wavelength range is far below the GaAs band gap of 1.42 eV, and the saturable absorption is believed to be realized by both the EL2 defect formed in the deep donor-level band gap and the nonlinear absorption process of GaAs under a high laser cavity intensity [12, 13]. Absorption at 1.06 μm in GaAs is attributed to photo-ionization of deep levels. These levels can be induced intentionally by doping with elements like Cr or arise from stoichiometric defects. In undoped GaAs, the primary defect is EL2, a donor level positioned approximately 0.8 eV below the conduction band edge. EL2 donors in undoped GaAs play a crucial role in providing charge compensation, enabling the growth of semi-insulating samples. Understanding the role of EL2 contributes to insights into absorption mechanisms and has implications

for controlled development of semi-insulating GaAs materials in semiconductor physics and technology. In 2 μm wavelength band, GaAs has been successfully used as SA in PQS Tm^{3+} -doped lasers [14, 15], the energy of laser photons in this context is approximately 0.61 eV, which is even lower than 1 μm laser photons. The absorption phenomenon can be attributed to the flexible nonlinear effects in GaAs material. It has been demonstrated that, under high cavity optical density, the two-photon absorption and free carrier absorption become dominant in the nonlinear process and promote the occurrence of the multi-photon absorption. The theoretical description of the multi-photon absorption process was first described by Maria Goppert-Mayer and Bobrysheva [16, 17]. The experimental multi-photon absorption characteristics of GaAs have been also investigated in mid-infrared spectral range [18]. The energy of laser photons generated in a Ho^{3+} -doped material is close to the Tm^{3+} -doped laser. Since the PQS Tm^{3+} -doped lasers based on GaAs has been realized, it is expected that the Ho^{3+} -doped PQS lasers with GaAs SA are also possible to be obtained.

GaAs is a semiconductor, whose band structure is complex and diverse for absorbing different types of photons. The photon energy in the 2 μm band is lower than the band-gap energy of GaAs, approximately 0.59 eV [18]. According to the multi-photon absorption theory, three-photon absorption happens, when the optical density inside the cavity is sufficient to surpass the band-gap energy [19, 20]. In this process, there exists a proportional relationship between the three-photon absorption coefficient and the intracavity energy [18].

In this paper, we demonstrate a 2 μm Ho:YAG ceramic laser, using GaAs SA. We discuss the three-photon absorption mechanism of GaAs at 2 μm wavelength. We achieve a maximum output power of 0.44 W at an absorbed pump power of 1.28 W, corresponding to a slope efficiency of 41.3%. With a 1907 nm Tm-doped fiber-laser-pump source, stable pulses of 114–295 kHz repetition rate are generated and the shortest pulse width, largest single pulse energy, and highest peak power are measured to be 83 ns, 1.49 μJ , and 17.95 W, respectively.

2. Experimental Setup

In this subject, we use a simple parallel resonator configuration. The schematic of the experimental setup is shown in Fig. 1. The pump source used in the experiment is a Tm-doped fiber laser comprising a 5 m length of double clad fiber, which can supply 5 W continuous-wave pump power. The central wavelength of the pump source is 1907 nm, the beam quality factor M_2 is 1.05, and the spectral line width is 0.7 nm. The pump laser beam is focused into the center of the Ho:YAG ceramic, using a 50 mm focal length lens L2, resulting in a 150 μm pump laser radius inside the ceramic. The rear mirror M1 is a dichroic mirror with high transmission coating at 1907 nm and high reflection coating ($\text{HR} > 99.7\%$) from 2000 to 2150 nm. The transmission rate of the output coupler is 10% from 1950 to 2150 nm. The

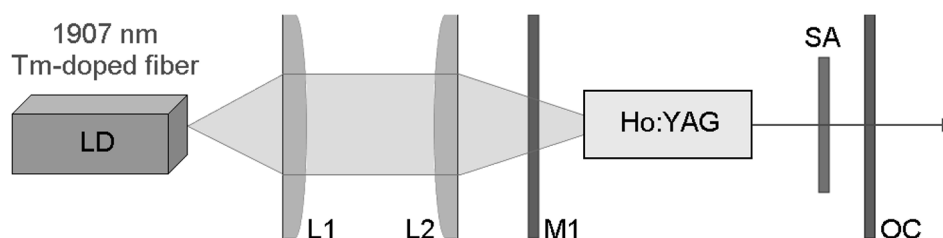


Fig. 1. Schematic of the experimental setup.

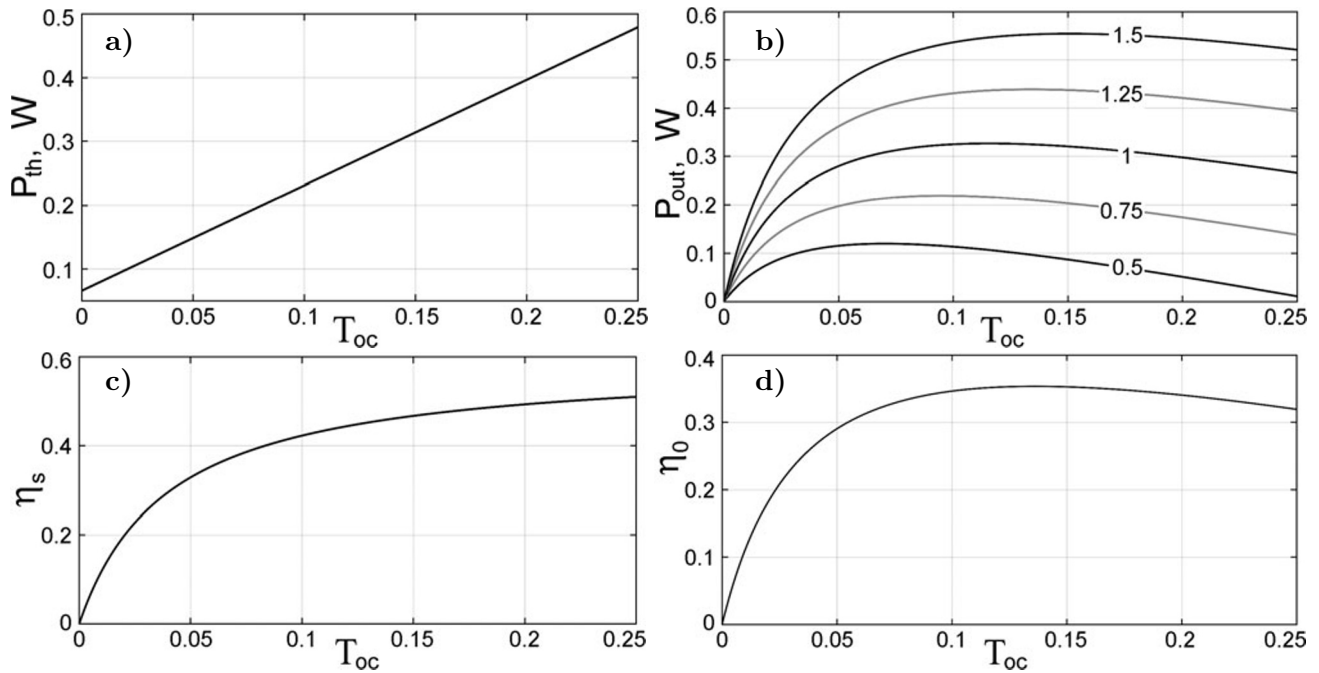


Fig. 2. Simulated threshold power (a), output power (b) (here, pumping power in W is written on the curves), slope efficiency (c), and optical conversion efficiency (d) at different output coupling transmittances.

size of the crystal is $3 \times 3 \times 4$ mm, installed in a 15°C water-cooled copper block. The SA is a $500 \mu\text{m}$ thick pure GaAs wafer without active cooling and optical coating.

3. Experimental Results and Discussions

To optimize our experiment, we first performed a data simulation. The results of the simulation are shown in Fig. 2, where the threshold power, output power, slope efficiency, and optical conversion efficiency are present at different output coupling transmittances. The slope efficiency, average output power, and optical conversion efficiency are basically saturated at 10% output coupling transmittance. Therefore, we select a 10% transmitted output coupler.

The relationship between the average output power and the power of the absorption pump is shown in Fig. 3. In the CW mode, the maximum output power is 0.67 W, the slope efficiency is measured to be 57.1%, and the corresponding absorption pump power is 1.28 W. In the PQS mode, the maximum average output power is 0.44 W, and the

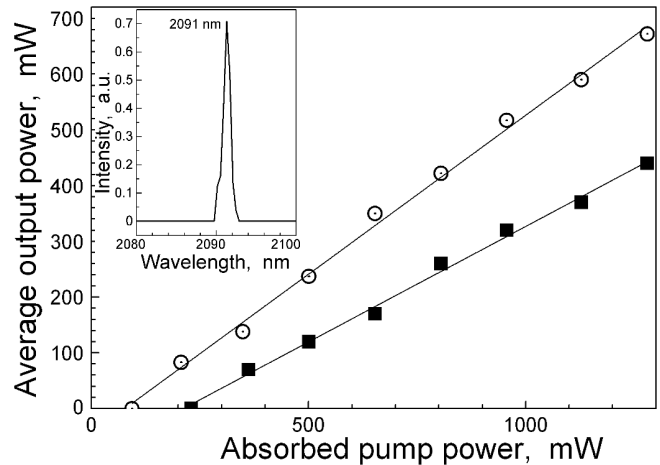


Fig. 3. Laser performance of the Ho:YAG ceramics laser with 10% transmission optical cavity (OC) in PQS (■) and continuous (⊙) modes; the inset shows the spectrum at the maximum PQS output power.

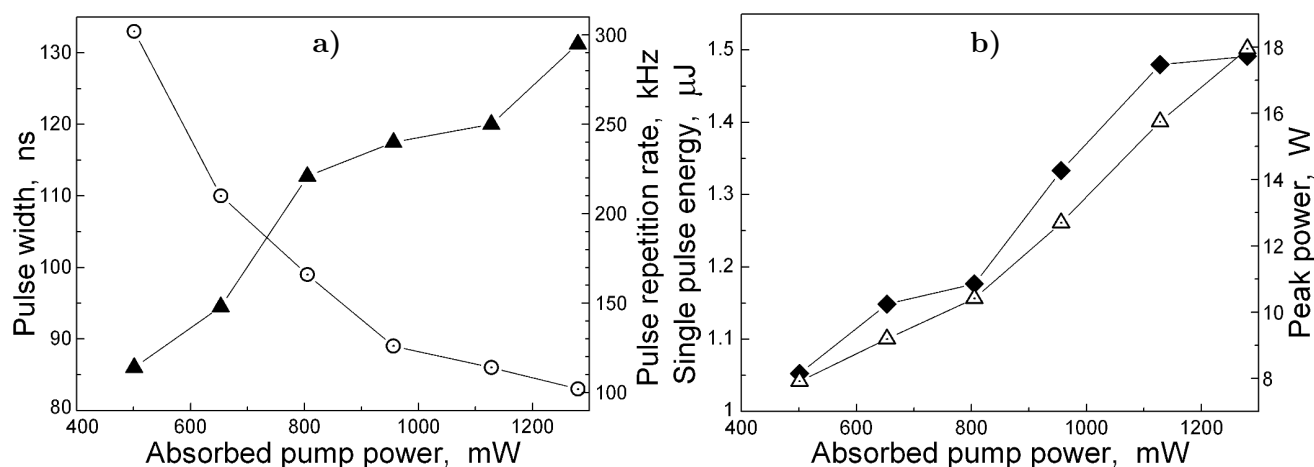


Fig. 4. The pulse width (\odot) and repetition rate (\blacktriangle) versus the absorbed pump power (a) and the single pulse energy (\blacklozenge) and peak power (\triangle) versus the absorbed pump power (b).

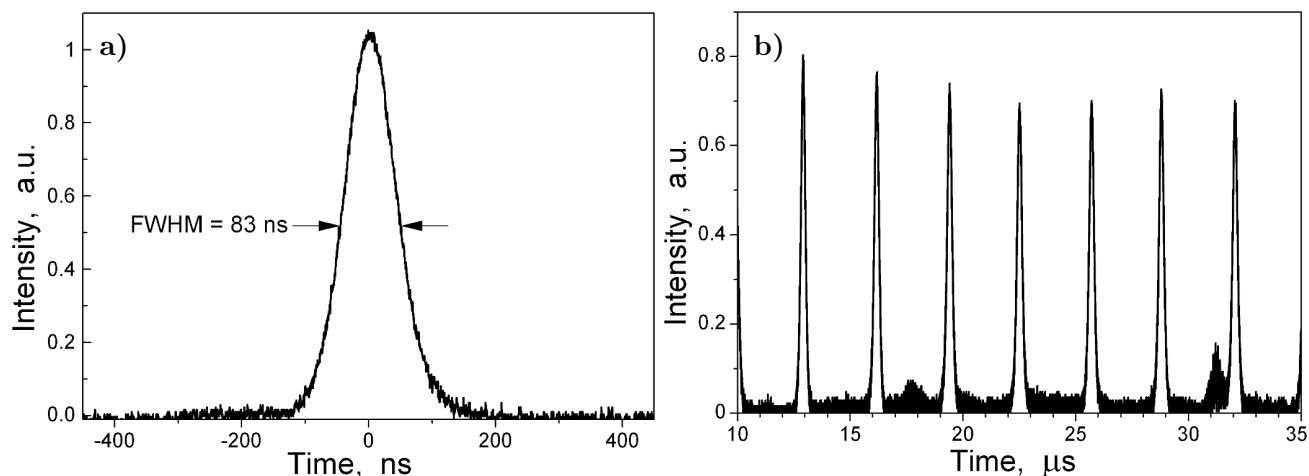


Fig. 5. The single pulse profile (a) and the pulse train at 1.28 W absorbed pump power (b). Here, the pulse repetition rate is 295 kHz.

slope efficiency is 41.3%. No power roll-off is observed, and the excellent linear dependence implied a further power scaling can be expected. The inset shows the output spectrum of the Ho:YAG ceramic laser at the maximum average output power in the PQS mode. The central wavelength is located at 2091.3 nm, and the spectral line width is about 1.0 nm.

The variation of repetition rate and pulse width at different pump powers is shown in Fig. 4 a. As the pump power increases, the pulse repetition rate continues to increase, and the pulse width decreases; the highest repetition rate and shortest pulse width are 295 kHz and 83 ns, respectively. In Fig. 4 b, we show the peak power and single pulse energy versus the absorbed pump power. As the pump power increases, the peak power almost linearly increases; the highest peak power and largest pulse energy are 17.95 W and 1.49 μJ , respectively.

In Fig. 5, we show the single pulse profile and the pulse train generated at an absorbed pump power of 1.28 W. The single pulse width is 83 ns, and the pulse train repetition rate is 295 kHz. The pulse train exhibits both fluctuations and timing jitter, which may be induced by the thermal load from the cavity.

4. Summary

We reported on a successful application of GaAs as a SA for the generation of nanosecond pulses near 2.1 μm , using Ho:YAG transparent ceramics as a gain medium. An average output power of 0.44 W at 2091 nm was obtained corresponding to a slope efficiency of 41.3%. The shortest pulse duration was 83 ns at a repetition rate of 295 kHz, and the pulse energy and peak power reached 1.49 μJ and 17.95 W, respectively. To the best of our knowledge, this is the first report of 2 μm Ho:YAG ceramic/GaAs PQS laser.

Acknowledgments

The authors acknowledge the financial support provided within the Natural Science Foundation of Shandong Province under Grant No. ZR2023MA046.

References

1. P. A. Budni, L. A. Pomeranz, M. L. Lemons, et al., *J. Opt. Soc. Am. B*, **17**, 723 (2000); DOI: 10.1364/JOSAB.17.000723
2. L. Wang, C. Gao, M. Gao, et al., *Opt. Express*, **22**, 254 (2014); DOI: 10.1364/OE.22.000254
3. R. Lan, P. Loiko, X. Mateos, et al., *Appl. Opt.*, **55**, 4877 (2016); DOI: 10.1364/AO.55.004877
4. J.-H. Yuan, B.-Q. Yao, X.-M. Duan, et al., *Optik*, **127**, 1595 (2016); DOI: 10.1016/j.ijleo.2015.11.043
5. X. M. Duan, Y. J. Shen, B. Q. Yao, and Y. Z. Wang, *Optik*, **169**, 224 (2018); DOI: 10.1016/j.ijleo.2018.05.094
6. A. Ikesue, T. Kinoshita, K. Kamata, and K. Yoshida, *J. Am. Ceram. Soc.*, **78**, 1033 (1995); DOI: 10.1111/j.1151-2916.1995.tb08433.x
7. W. X. Zhang, J. Zhou, W. B. Liu, et al., *J. Alloys Compd.*, **506**, 745 (2010); DOI: 10.1016/j.jallcom.2010.07.059
8. J. Lu, T. Murai, K. Takaichi, et al., *Appl. Phys. Lett.*, **78**, 3586 (2001); DOI: 10.1063/1.1378053
9. J. Yuan, B. Yao, T. Dai, et al., *Laser Phys.*, **30**, 035004 (2020); DOI: 10.1088/1555-6611/ab70b4
10. B. Yao, Y. Tian, G. Li, and Y. Wang, *Opt. Express*, **18**, 13574 (2010); DOI: 10.1364/OE.18.013574
11. L. Liu, H. Chu, X. Zhang, et al., *Nanoscale Res. Lett.*, **14**, 112 (2019); DOI: 10.1186/s11671-019-2953-7
12. A. L. Smirl, G. C. Valley, K. M. Bohnert, and T. F. Boggess, *IEEE J. Quantum Electron.*, **24**, 289 (1988); DOI: 10.1109/3.125
13. J. Liu, X. Chen, W. Han, et al., *IEEE Photonics Technol. Lett.*, **28**, 1104 (2016); DOI: 10.1109/LPT.2016.2531670
14. C. Kieleck, A. Hildenbrand, M. Eichhorn, et al., *Proc. SPIE*, **7836**, 783607 (2010); DOI: 10.1117/12.865217
15. L. Wu, D. Li, S. Zhao, et al., *Opt. Express*, **23**, 15469 (2015); DOI: 10.1364/OE.23.015469
16. P. T. So, "Two Photon Fluorescence Light Microscopy," in eLS, John Wiley & Sons (2001); DOI: 10.1038/npg.els.0002991
17. A. Bobrysheva and S. Moskalenko, *Fiz. Tekh. Poluprovodn.*, **3**, 1601 (1969) [in Russian].
18. W. C. Hurlbut, Y.-S. Lee, K. L. Vodopyanov, et al., *Opt. Lett.*, **32**, 668 (2007); DOI: 10.1364/OL.32.000668
19. A. Villeneuve, C. C. Yang, G. I. Stegeman, et al., *IEEE J. Quantum Electron.*, **30**, 1172 (1994); DOI: 10.1109/3.303676
20. O. H. Heckl, B. J. Bjork, G. Winkler, et al., *Opt. Lett.*, **41**, 5405 (2016); DOI: 10.1364/OL.41.005405